Journal of Biomolecular NMR, 10 (1997) 255–262
KLUWER/ESCOM

J-Bio NMR 467

Measurement of diffusion constants for nucleic acids by NMR

Jon Lapham, Jason P. Rife, Peter B. Moore and Donald M. Crothers*

Department of Chemistry, Yale University, P.O. Box 208107, New Haven, CT 06520-8107, U.S.A.

Received 14 April 1997
Accepted 22 May 1997

Keywords: Translational self-diffusion; Spin echo; Pulsed field-gradient; Hairpin; Duplex

Summary

Pulsed field-gradient NMR experiments can be used to measure the diffusion constants of nucleic acids. The diffusion constants measured in this way for double-helical DNAs of defined length agree well both with theory and with measurements done using other techniques. When applied to RNAs, this experiment easily distinguishes duplex RNAs from RNA hairpins and thus it can solve one of the perennial problems faced by RNA spectroscopists, i.e. assessing whether their samples are monomeric or not.

Introduction

The rate at which individual DNA and RNA molecules move through solution, i.e. the translational self-diffusion rate, is of fundamental importance for many important aspects of nucleic acid biochemistry. Any process which changes the apparent hydrodynamic parameters of a nucleic acid, such as protein or ligand binding, drug intercalation, or bending, can produce a measurable change in this diffusion rate.

The NMR pulsed field-gradient (PFG) spin-echo technique (Hahn, 1950; Stejskal and Tanner, 1965) has long been used to measure diffusion constants. Applications to biological systems include determination of the aggregation state of proteins (Altieri et al., 1995; Dingley et al., 1995), measurement of the bulk movement of hemoglobin in human erythrocytes (Kuchel and Chapman, 1991) and quantitation of processes such as amide proton exchange with water (Andrec and Prestegard, 1996). For NMR spectroscopists, it provides a simple, accurate method for measuring the diffusion constants of the materials they are investigating under the same conditions as other NMR experiments they do. The results of application of this technique to DNA and RNA are presented here, and are compared to those obtained by other methods and to the predictions from theory.

The ability to affirm that RNA samples are monomeric is of paramount importance for NMR spectroscopists performing structural studies on short RNA oligonucleotides. The spectrum of a hairpin can often be similar to that of the duplex, formed from the same sequence, due to the inherent symmetry of dimerization. Many experiments have been utilized to investigate this problem: monitoring the hyperchromic UV shift of melting (Marky and Breslauer, 1987; Cheong et al., 1990; Heus and Pardi, 1991), native polyacrylamide gel electrophoresis (Sen and Gilbert, 1992), NMR T_1/T_2 relaxation measurements, and ^{15}N isotope-filtered NOESY experiments (Aboul-ela et al., 1994; Sich et al., 1996). Many of the possible non-NMR experiments must either be done in buffers different from those used for NMR or that are incompatible with the high RNA concentrations required for NMR. The T_1/T_2 relaxation measurement can be difficult to implement, especially in the 2D heteronuclear NMR experiments, and may be complicated by dynamics which are independent of the aggregation state of the RNA. The ^{15}N X-filtered NOESY experiment developed by Aboul-ela provides a general solution to the problem, but it requires the labor-intensive synthesis of isotope-labeled RNA, and the mixing of precious labeled RNA with unlabeled RNA.

It should be possible to discriminate between an RNA hairpin and the corresponding self-dimer by measuring the translational self-diffusion rates. In the case of short oligonucleotides, it is often possible to drive the hairpin to duplex equilibrium by increasing strand concentration

*To whom correspondence should be addressed.

and salt concentration, which makes it possible to compare the two states. Additionally, by selecting the appropriate hydrodynamic model for the RNA, it should be possible to predict the diffusion rates for both states. Further analysis and comparison of the diffusion rate of a variety of RNAs may yield structural insights into their molecular shapes.

Theory

The translational self-diffusion coefficient (D_t) for a molecule in solution is related to its translational frictional coefficient (F_t) by Einstein's equation:

$$D_t = kT/f_t \quad (1)$$

Thus, an accurate calculation of D_t is equivalent to an accurate calculation of a frictional coefficient. Frictional coefficients are usually computed assuming that the hydrodynamic shape of a molecule is a sphere, a prolate (or oblate) ellipsoid or a symmetric cylinder. While it seems obvious that the best model for a duplex nucleic acid would be a symmetric cylinder, given the sizes of the nucleic acids that we studied (a 14 nucleotide RNA hairpin to a 24 base pair (bp) DNA), we also investigated modeling them as spheres or ellipsoids.

The spherical model for nucleic acids is probably accurate for either short duplexes or short hairpins. In this case,

$$f_t = 6\pi\eta r \quad (2)$$

where r is the hydrodynamic radius of the sphere and η is the viscosity of the solvent.

As the length of the nucleic acid duplex increases, prolate ellipsoid models may be more successful. In this case, the Perrin equations (Cantor and Schimmel, 1980) can be used:

$$f_t = 6\pi\eta_0(ab^2)\left[\frac{(1-p^2)^{1/2}}{p^{2/3}}\right]\ln\left\{\left(1+(1-p^2)^{0.5}\right)/p\right\} \quad (3)$$

where a is defined as half the length of the long axis and b as half the length of the short axis for an ellipse. The axial ratio, p, is b/a.

Expressions for the frictional coefficient for a short symmetric cylinder model were developed by Tirado and Garcia de la Torre (1979,1980) which are appropriate for short rod-like molecules with $2<q<30$, where q is the axial ratio defined as a/b:

$$f_t = 6\pi\eta_0\left[\frac{L/2}{\ln q + 0.312 + 0.565q^{-1} - 0.100q^{-2}}\right] \quad (4)$$

This expression is known to work well for DNA dimers of moderate size (Eimer et al., 1990).

NMR theory

Stejskal and Tanner (1965) first proposed a spin-echo experiment to measure the diffusion rate of molecules in solution by NMR. Their method relies on two gradient pulses surrounding the 180° pulse in the spin echo: the first dephases the transverse magnetization in a spatially dependent manner along the z-axis and the second gradient then rephases the magnetization. If the molecule moves along the z-axis during the time between the two gradients, its magnetization will not refocus completely. Thus, if the molecule diffuses rapidly, the attenuation of its resonances will be large; if the molecule diffuses slowly, the attenuation will be relatively small. The following relation exists between translational self-diffusion and the measurable NMR parameters (Stejskal and Tanner, 1965):

$$A/A_0 = -\exp[D_t\gamma_H^2\delta^2G_z^2(\Delta - \delta/3)] \quad (5)$$

where A is the measured peak intensity (or volume), A_0 is the maximum peak intensity, D_t is the translational diffusion constant (in cm^2/s), γ_H is the gyromagnetic ratio of a proton (2.675197×10^4 G^{-1} s^{-1}), δ is the duration of the gradient, Δ is the time between gradients and G_z is the strength of the gradient (in G/cm). Data can be plotted as $-\ln(A/A_0)$ versus $\gamma_H^2\delta^2G_z^2(\Delta-\delta/3)$. The slope of the line that emerges is D_t.

Materials and Methods

Sample preparation

All the DNA samples were prepared on an Applied Biosystems 380B DNA synthesizer and purified using denaturing PAGE techniques. Concentrations were determined by UV absorbance measurements at 260 nm wavelength and calculated using a dinucleotide stacking extinction coefficient formula. The DNA sequences were (5' to 3') D12:CGCGAATTCGCG, D14:GCTATAAAAAGGGA (with the complement TGCCCTTTTTATAGC) and D24:CGCGAATTCGCGCGCGAATTCGCG. Both D12 and D24 were palindromic to alleviate any problems with stoichiometry. Five D12 samples were prepared: 250, 500, 1000, 1500 and 2000 μM. Four D14 samples were prepared: 250, 500, 1200 and 2000 μM. Four D24 samples were prepared: 250, 500, 1000 and 1500 μM. All samples were dialyzed against 20 mM sodium phosphate (pH 7.0) and 100 mM NaCl for 2 days, exchanging the dialysis buffer every 12 h. All samples were placed in a Shigemi (Shigemi Corp., Tokyo, Japan) NMR tube in a 170 μl volume, which equated to about a 1 cm sample height. The samples were then lyophilized and resuspended in 100.0 atom% D_2O from Aldrich (cat #26,978-6) to the same final sample volume of 170 μl.

The RNA sequence was (5' to 3') R14:GGACCGGAAGGUCC and was prepared enzymatically using DNA

template-directed T7 RNA polymerase (Milligan et al., 1987), and purified using denaturing PAGE techniques. The RNA was extensively dialyzed against water, concentrated, and exchanged into either a low salt buffer (50 mM NaCl, 5 mM cacodylate, pH 6.3, 0.1 mM EDTA) or a high salt buffer (400 mM NaCl, 5 mM cacodylate, pH 6.3, 0.1 mM EDTA) using 1000 MWCO centrifugal concentrators (Filtron Technology Corp., Northborough, MA, U.S.A.). Both samples were heated to 80 °C, cooled to room temperature, placed in a Shigemi NMR tube with a sample volume of 160 µl, lyophilized, and 100.0 atom% D_2O was added to give a final sample volume of 160 µl. The final RNA 'strand' concentrations were 1.8 and 2.0 mM for the low salt (R14ls) and high salt (R14hs) samples, respectively. The R14ls and R14hs samples were proven to consist of a single species by means of standard homonuclear and heteronuclear experiments. For example, the number of H5-H6 cross peaks found in a DQF-COSY experiment corresponds to the number of pyrimidines in the sequence. We assume that the differences in the spectra between the two samples are due to a simple hairpin to duplex transition.

Solvent viscosity

All the methods discussed for modeling nucleic acid frictional coefficients require an accurate measure of the solvent viscosity, which was calculated from (Kellomaki, 1975; Natarajan, 1989)

$$\log \eta_0 = a + \left[\frac{b}{c - T}\right] \tag{6}$$

where T is the temperature in Kelvin. The terms a, b and c are given for a particular D_2O:H_2O ratio. For a 100% D_2O solution, a = –4.2911, b = –164.97 and c = 174.24. This yields a value of η_0 at 25 °C for a 100% D_2O solution of 1.097 kg/(cm s), which is what we used in our calculations. For a 100% H_2O solution, a = –4.5318, b = –220.57 and c = 149.39. This yields a value of η_0 at 25 °C for a 100% H_2O solution of 0.8929 kg/(cm s).

Corrections for salt effects on viscosity were performed as follows (Harned and Owen, 1958):

$$\eta = \eta_0[1 + A\sqrt{c} + B(c)] \qquad A = 0.0067,\ B = 0.0244 \text{ (for NaCl)} \tag{7}$$

where c is the molar salt concentration, η_0 is the zero solute solvent viscosity and η is the new viscosity. We found that for the range of NaCl used in this study (50–400 mM) the effect on viscosity was very small, with the largest viscosity correction being $1.014\eta_0$ for the 400 mM NaCl case.

NMR calibration

It is absolutely critical to the interpretation of these experiments that the gradient hardware and probe be calibrated. This was done using a 1 cm high sample of 100% D_2O in a Shigemi NMR tube. Necessary calibrations include measurement of the maximum strength of the gradient pulse, characterization of the eddy-current recovery time for the probe, and examination of the linear power response of the z-axis gradients. We found that many of our older probes did not behave properly in these tests, and they were not used. This is probably because the electronics of the older probes are not as well shielded from the gradient pulse.

Calibration of the gradient strength was accomplished by two methods. The first, which has been previously published (Callaghan et al., 1983), involves measuring the diffusion rate for the residual proton water line in the calibration sample at 25 °C, and back-calculating G_z. This procedure assumes that the diffusion rate for HDO in a 100% D_2O sample is 1.90×10^{-5} cm^2/s (Longsworth, 1960). The second depended on acquiring a spin-echo FID of the calibration sample with the z-axis gradient on during acquisition. This yields a spatial profile of the sample, which is a function of the sample height and the gradient strength. Slightly different values for G_z were obtained by these two methods of calibration. The discrepancy was within 3%, and similar to the gradient strength calibration errors reported elsewhere (Doran and Décorps, 1995).

The eddy-current recovery time was examined using a pulse sequence in which a full-strength gradient pulse is applied for 10 ms (a longer time than is used in the experiments) followed by an adjustable time delay and finally a 90° proton observation pulse. Data were collected on the residual proton water line in the calibration

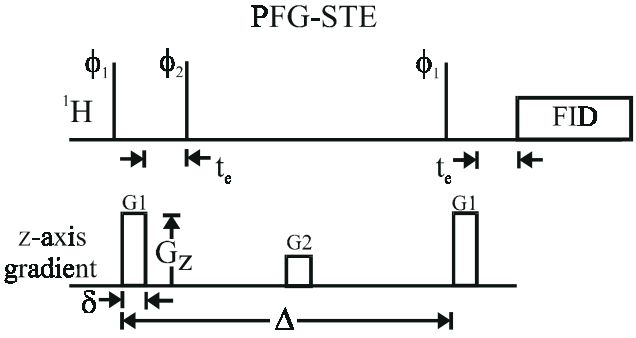

Fig. 1. PFG-STE (Tanner, 1970) pulse sequence for the diffusion measurements. δ refers to the length of the first and third gradient pulse, Δ is the time between the first and third gradient pulse and G_z is the strength of the G1 gradient pulse. One experiment would involve choosing a particular δ and Δ value (between 1 and 5 ms for δ and between 25 and 200 ms for Δ), and collecting 31 1D spectra in which the value of G_z is incremented from 1 to 31 G/cm. The middle gradient (G2) pulse is a spoiler to remove any unwanted transverse magnetization during the z-axis storage. The time t_e is the time for complete eddy-current relaxation, and must be calculated independently for each hardware setup; we used a delay of 2 ms. The phase cycling was as follows: ϕ_1 (x,–x,–y,y), ϕ_2 (–x,x,y,–y), the receiver was the same as ϕ_2.

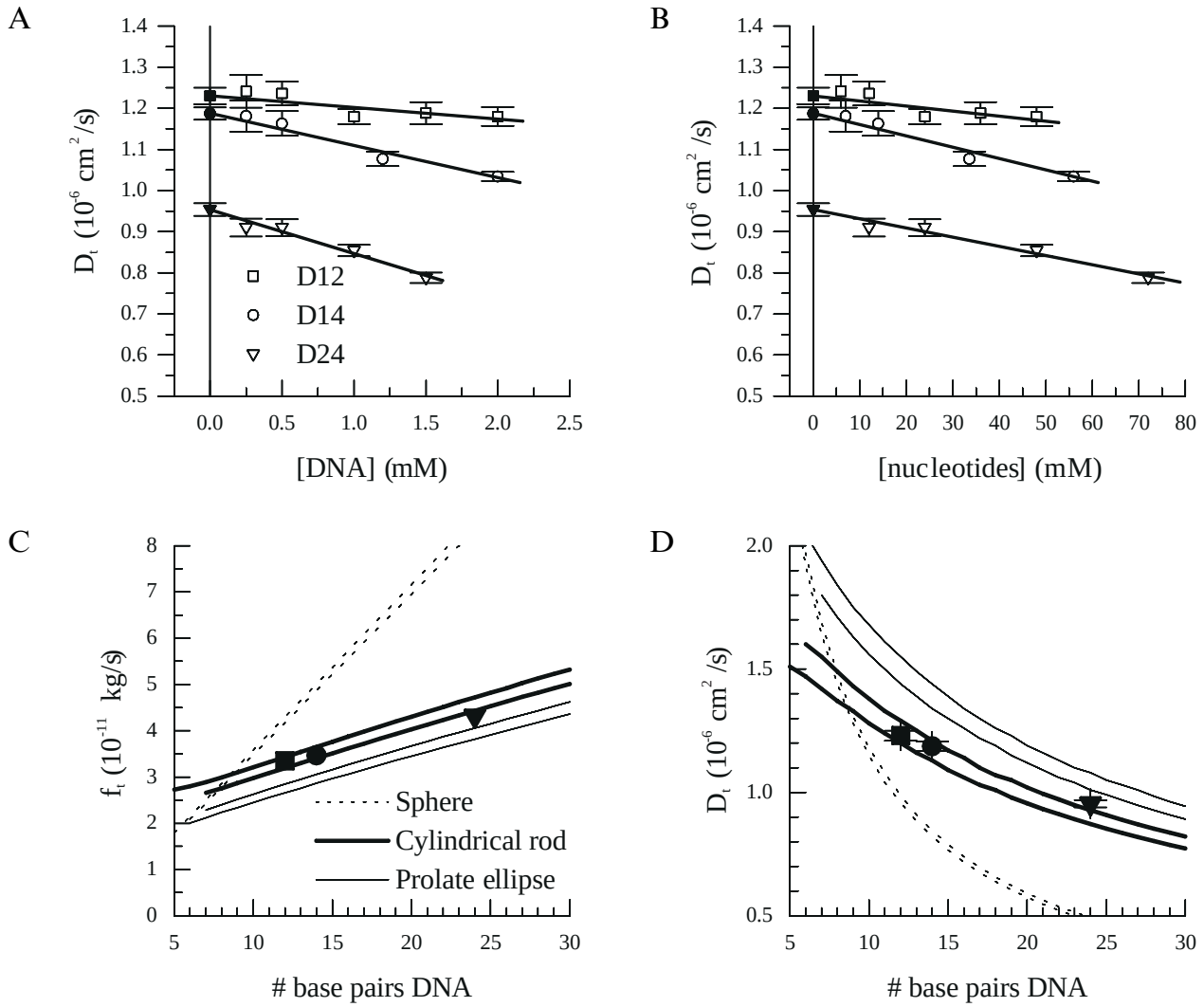

Fig. 2. (A) A plot of the concentration dependence (D_t versus [DNA]) of the measured diffusion rate for the D12, D14 and D24 samples. The experimental data are represented by open squares, open circles and open diamonds for each sample respectively. The extrapolated 'zero-concentration' values are shown as solid symbols. (B) The same data as in (A), but plotting D_t versus nucleotide concentration. (C) Graph of the theoretically calculated translational friction coefficients for a sphere (between the dotted lines), ellipse (between the thin lines) and cylindrical top (between the thick lines) at 25 °C in 100% D_2O as a function of DNA base pair length, using the hydrodynamic parameter range of 3.4(±0.5) Å rise/bp and a diameter of 20(±1.0) Å. The lines for the cylindrical rod and prolate ellipsoid do not extend completely to the y-axis because they cannot be calculated for those values of p. (D) Graph of the theoretically calculated translational diffusion constant.

sample. It was found that there was complete eddy-current relaxation within less than 1 ms for the triple-resonance probe used in these experiments. Because of this, we simply needed to wait longer than 1 ms after applying the gradients in the stimulated echo (PFG-STE) sequence.

It is absolutely critical for these experiments that the z-axis gradients be linear in the volume occupied by the sample, and respond linearly to the power applied. The region of linearity may only be a little larger than 1 cm in typical gradient-equipped probes, so an accurate measurement requires that the sample height be no larger than this. Measurements were made using the PFG-STE sequence of the residual proton line in the calibration sample over a large range of δ and Δ times. The data gave the same D_t value for each value of δ and Δ, and the plot of $-\ln(y/y_0)$ versus $\gamma^2\delta^2G_z^2(\Delta-\delta/3)$ was a straight line, which demonstrates the linear gradient power response required.

NMR experimental

All the DNA data were collected on a Varian 600 MHz 'UnityPlus' spectrometer on a triple-resonance (H, C, N) probe. The PFG-STE pulse sequence shown in Fig. 1 was used for all the data reported. However, we also collected data using the simple PFG spin-echo and the Longitudinal Eddy-current Delay (PFG-LED) pulse sequences, and obtained similar results. A post gradient eddy-current relaxation delay of 2 ms was used on all experiments. For the 1000–2000 μM samples, 32 scans were collected at each gradient strength reported; how-

ever, for the lower concentration samples, more scans were needed to obtain reasonable signal to noise values, up to 256 scans for the most dilute 250 μM samples. For each data set, 2048 complex points were collected for each of 32 experiments in which the gradient strength was incremented from 1 to 31 G/cm in steps of 1 G/cm. A 5 s recycle delay was used between scans for all data shown. However, data were also collected using a range of recycle delays from 1 to 10 s, with no apparent change in the measured diffusion rate.

The region of the spectrum from 8.5 to 7.0 ppm (which corresponds to the H8/H6/AH2 protons in DNA and RNA) or the region from 6.0 to 5.0 ppm (corresponding to the H1'/H5 protons in DNA and RNA) was integrated for each data set. Spectra were processed using the Felix95 (Biosym Technologies, San Diego, CA) software package using an automated processing macro which apodized the FID, Fourier transformed the data, applied baseline correction, integrated the peaks and saved a volume file for each experiment. These data were then plotted as $-\ln(A/A_0)$ versus $\gamma_H^2\delta^2G_z^2(\Delta-\delta/3)$ (see Fig. 4 for an example) in which the slope of the line gives the translational self-diffusion rate of the molecule for a particular concentration.

Results

NMR experimental

A number of variants of the original PFG spin-echo pulse sequence have been developed for measuring diffusion rates. A PFG-STE pulse sequence (see Fig. 1) was developed by Tanner (1970) which makes use of three 90° pulses and stores magnetization along the z-axis (minimizing T_2 relaxation effects) during a large portion of the experiment. It works well for studying molecules with $T_1 > T_2$, such as large biomolecules. The inductive eddy-current magnetic field-gradients created in the electronics of probes can affect the line shapes of resonances in PFG experiments. Many variants to the PFG-STE have been developed to minimize these effects. A refocused stimulated echo sequence was developed by Griffiths and Horton (1990) in which a train of refocusing 180° pulses is applied at the end of the standard PFG-STE as well as a four-pulse sequence with a PFG-LED (Gibbs and Johnson, 1991) which allows for an extra delay time before acquisition. Shaped gradient pulses (Price and Kuchel, 1991) have also been used. A water suppression component has been included in the water-suppressed LED (water-sLED) pulse sequence (Altieri et al., 1995).

We found that, for our hardware, the relaxation time required for the gradient-induced eddy currents to decay to zero was short enough so as to not be a factor (see the 'NMR calibration' section). For this reason, we utilized the simpler technique of Tanner's three-pulse 'z-storage' PFG-STE pulse sequence. Many of the more complex eddy-current suppression pulse sequences just mentioned were also implemented, but they did not affect the quality of the data.

DNA

The three DNA duplexes studied (12, 14 and 24 base pairs) were prepared in concentrations ranging from 250 to 2000 μM to examine the effect of DNA concentration on the translational self-diffusion rate. Figure 2 summarizes the results. It is clear that there is indeed a concentration dependence, with the apparent diffusion rate being lower for high concentration samples (Fig. 2A). This is presumably because intermolecular repulsion restricts the volume available for diffusion. Furthermore, the concentration dependence effect is more pronounced for the longer samples: D24 shows an almost 20% decrease in diffusion rate between the 250 and 1500 μM sample, while D12 shows only an ~5% decrease over the same concentration range. Figure 2B demonstrates that plots of D_t versus nucleotide concentration give more nearly equal slopes between samples. A simple linear virial correction to the measured self-diffusion rate,

$$D_t(\text{measured}) = D_0(1 + kc) \quad (8)$$

describes this concentration dependence quite well (see Table 1 for values of k). The diffusion constants of DNAs at zero concentration were determined by linear regression of the data plotted in Fig. 2B, and the values are reported in Table 1. The theoretical f_t and D_t values calculated for DNAs varying in size from 5 to 35 base pairs are graphed in Figs. 2C and D along with the measured D_t (and back-calculated f_t) values. Clearly, the Tirado

TABLE 1
THEORETICAL AND EXPERIMENTAL SELF-DIFFUSION CONSTANTS[a]

Size	Theoretical (10^{-6} cm^2/s)	Experimental D_t (10^{-6} cm^2/s)	k (10^{-3} cm^2/(s mM)
D12	1.247	1.230 (0.020)	−1.4 (0.4)
D14	1.170	1.187 (0.015)	−2.7 (0.2)
D24	0.903	0.954 (0.015)	−2.2 (0.2)
R14ls[b]	1.90	1.41 (0.014)	
R14hs[c]	1.16	0.918 (0.024)	

[a] Values were calculated using the rigid cylindrical rod model at 25 °C and 100% D_2O. For DNA, the hydrodynamic parameters of 3.4 Å rise/bp and 20 Å diameter were used. For RNA, 2.6 Å rise/bp and 24 Å diameter were used. Experimental D_t values for the DNA come from extrapolation to zero concentration. k is the virial coefficient in Eq. 8, using concentration units of mM nucleotide (not strand) concentration.

[b] R14ls was modeled as a sphere with a radius of 21 Å (as discussed in the text) and the reported D_t value was not corrected for concentration, [R14ls] = 1.8 mM.

[c] R14hs was modeled as a rigid cylinder using the hydrodynamic parameters of 2.6 Å rise/bp and 24 Å diameter and the experimental D_t value was not corrected for concentration, [R14hs] = 2.0 mM.

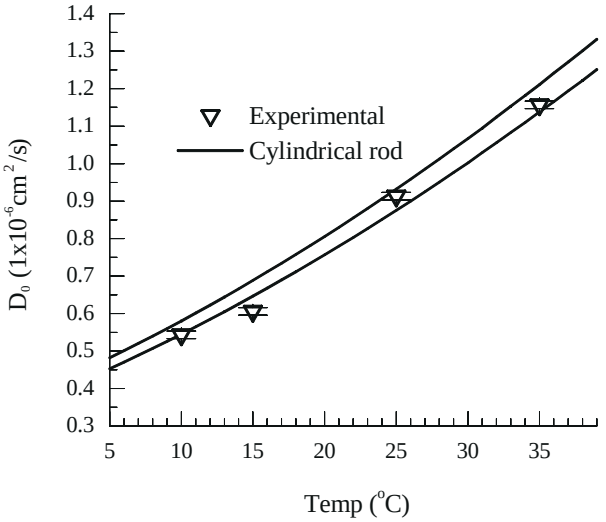

Fig. 3. Graph of diffusion constant versus temperature. Solid lines represent the theoretically calculated diffusion rate using the cylindrical rod method with 3.4(±0.5) Å rise/bp and 20.0(±1.0) Å diameter. Data were collected on D24 at 1.5 mM concentration (72 mM nucleotide concentration); the results shown were corrected for concentration using $k = -2.2 \times 10^{-3}$ cm^2/(s mM).

and Garcia de la Torre symmetric cylindrical model fits the DNA data the best.

The temperature dependence of D_t for the DNA was examined by collecting data on D24 at temperatures ranging from 10 to 50 °C. Equation 1 predicts direct proportionality between D_t and temperature; however, the temperature dependence of viscosity must also be calculated (using Equ. 6). Figure 3 graphs the theoretically predicted temperature dependence of a 24 bp DNA (using the parameters of 3.4(±0.5) Å rise/bp and 20.0(±1.0) Å diameter), overlaid with the experimentally measured values (corrected for DNA concentration). Data are only shown to 35 °C, because at higher temperatures the gradients did not give a linear response and reliable data could not be obtained.

Data were collected on D12 at three NaCl ion concentrations (50, 100 and 200 mM) to examine the effect this might have on our reported D_t values. There was no appreciable change in the measured D_t values outside experimental error (data not shown). Fujimoto et al. (1994) have measured the dependence of the hydrodynamic radius (R_H) of a 48 bp DNA on cation concentrations using fluorescence polarization anisotropy (FPA) of intercalated ethidium. They found that NaCl concentration had the smallest effect of any of the cations examined, decreasing R_H by 0.30 Å from [NaCl] = 25 mM to 100 mM. Other cations such as Mn^{2+} and Mg^{2+} gave rise to much larger changes in R_H. Our data seem to be in agreement with what they report.

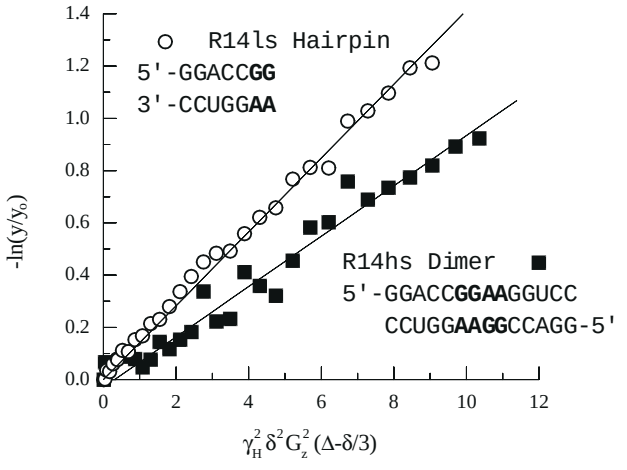

Fig. 4. Diffusion measurements at 25 °C for the low salt hairpin R14ls (1.8 mM strand concentration, 25.2 mM nucleotide concentration) and the high salt duplex R14hs (2.0 mM strand concentration, 28 mM nucleotide concentration). The sequences of the RNA are shown, with the hairpin loop and internal loop regions represented by the bold letters.

RNA

The RNA studied, R14, could be examined either as a hairpin or a duplex because its conformation depends on the NaCl concentration. Under the conditions of low salt (100 mM NaCl), the RNA (R14ls) is a hairpin with the approximate hydrodynamic dimensions of L = (2.6 Å rise/bp) × 7 bp = 18.2 Å and D = 24 Å (Arnott and Hukins, 1973). Assuming a sphere of radius 18–24 Å, the range of D_t predicted is 2.19×10^{-6} to 1.66×10^{-6} cm^2/s using Eq. 2. With an the average radius value of 21 Å, the theoretical D_t is 1.90×10^{-6}. The rationale for modeling R14ls as a sphere comes from the observation (Eimer, 1990) that a DNA tridecamer which adopted a hairpin structure was nearly spherical in its hydrodynamic dimensions. By analogy the RNA tetradecamer hairpin should adopt a nearly spherical structure. Under the conditions of high salt (400 mM NaCl), the duplex RNA (R14hs) can be modeled as a right cylinder of dimensions L = 36.4 Å and D = 24 Å, which gives a theoretical D_t of 1.16×10^{-6} cm^2/s from Eq. 4. The ratio of the theoretically calculated D_t(duplex): D_t(monomer) is 0.61.

The data obtained for R14ls and R14hs are shown graphically in Fig. 4. The diffusion constants obtained were $1.41(0.014) \times 10^{-6}$ and $0.918(0.024) \times 10^{-6}$ cm^2/s for the monomer and duplex respectively. These values were not corrected for concentration effects. This gives an experimentally calculated D_t(duplex):D_t(monomer) ratio of 0.65, in close agreement with the predicted ratio of the diffusion rates for a duplex:monomer.

Discussion and Conclusions

DNA: Comparison to other techniques

The hydrodynamic parameters of length and diameter appropriate for double-helical DNA have long been debated. Fiber diffraction studies of high-humidity B-form

DNA suggest a phosphate to phosphate diameter for DNA of 20 Å (Arnott and Hukins, 1972; Elias and Eden, 1981). However, the hydrodynamic diameter should include any associated water that moves with the DNA. Our laboratory has reported a hydrodynamic radius of 22–26 Å and 3.34 ± 0.1 Å rise/bp for B-form DNA (Mandelkern et al., 1981) based on a combination of quasi-elastic light scattering and birefringence rise/decay of electric-field-oriented molecules in the size range of 64–267 base pairs. Measurements of large fragments must be corrected for the bendability of DNA, which was accomplished by Mandelkern et al. (1981) by extrapolation to zero bendability with the help of a theoretical model (Hearst, 1963).

Smaller DNA fragments do not require such an extrapolation and should thus be better model compounds for study. Measurements of translational and rotational diffusion rates by dynamic light scattering and NMR relaxation on short fragments (8, 12 and 20 base pairs) of DNA have given values of 20.0(±1.0) Å for the hydrodynamic diameter and a value of 3.4(±0.05) Å rise/bp (Eimer et al., 1990; Eimer and Pecora, 1991), and indicate that there may not be a water shell which diffuses with the DNA. These experiments were performed in 50 mM phosphate buffer, pH 7, 100 mM NaCl, 2 mM EDTA, 0.1% NaN_3 and in 100% H_2O. The D_t reported for each at 20 °C was 1.52, 1.34 and 1.09×10^{-6} cm^2/s for the 8-, 12- and 20-mer, respectively. The only direct comparison we can make with the data of Eimer and co-workers is for our 12-mer DNA, and our values are in very close agreement, after making the appropriate corrections for both the viscosity differences between H_2O and D_2O and the temperature differences between the two sets of data. We find that the hydrodynamic values they calculate work well for predicting our data as well. A possible reason for the larger hydrodynamic radii (diameter 22–26 Å versus 20 Å) inferred for DNA molecules of restriction fragment size (Mandelkern et al., 1981) is the presence of small amounts of intrinsic curvature in such samples.

RNA

In both RNA hairpin and the duplex measurements, our experimentally determined diffusion constants are less than those predicted (see Table 1). There are several reasons for this. First, we have not made any concentration correction. Second, the hairpin and a duplex containing an internal loop may be poorly represented using standard A-form helical parameters for diameter and rise/bp. Nevertheless, the similarity between the diffusion constant ratios for the theoretical (0.61) and experimental (0.65) values indicates that hairpin and helical dimers can be clearly distinguished. The analogy is in using diffusion constants to determine the aggregation states of proteins (Altieri et al., 1995; Dingley et al., 1995) when perfect hydrodynamic models are not known.

To summarize, a simple, accurate and quick experiment is presented for determining the translational self-diffusion constants of nucleic acid samples under NMR conditions. These data demonstrate that the PFG-STE technique gives accurate results for double-helical standard B-form DNAs, and can be used to determine whether an RNA sample is monomeric.

Acknowledgements

J.L. would like to thank Daniel P. Zimmer for the use of his D14 NMR sample. This work was supported by grants from the National Institutes of Health to D.M.C. (GM21966) and P.B.M. (GM41651).

References

Aboul-ela, F., Nikonowicz, E.P. and Pardi, A. (1994) *FEBS Lett.*, **347**, 261–264.

Altieri, A.S., Hinton, D.P. and Byrd, R.A. (1995) *J. Am. Chem. Soc.*, **117**, 7566–7567.

Andrec, M. and Prestegard, J.H. (1996) *J. Biomol. NMR*, **9**, 136–150.

Arnott, S. and Hukins, D.W.L. (1972) *Biochem. Biophys. Res. Commun.*, **47**, 1504.

Arnott, S. and Hukins, D.W.L. (1973) *J. Mol. Biol.*, **81**, 93–105.

Berne, B.J. and Pecora, R. (1976) *Dynamic Light Scattering*, Wiley, New York, NY, U.S.A.

Callaghan, P.T., Gros, M.A.L. and Pinder, D.N. (1983) *J. Chem. Phys.*, **79**, 6372–6381.

Cantor, C.R. and Schimmel, P.R. (1980) *Part II: Techniques for the Study of Biological Structure and Function*, Freeman, New York, NY, U.S.A.

Cheong, C., Varani, G. and Tinoco Jr., I. (1990) *Nature*, **346**, 680–682.

Dingley, A.J., Mackay, J.P., Chapman, B.E., Morris, M.B., Kechel, P.W., Hambly, B.D. and King, G.F. (1995) *J. Biomol. NMR*, **6**, 321–328.

Doran, S.J. and Décorps, M. (1995) *J. Magn. Reson.*, **A117**, 311–316.

Eimer, W., Williamson, J.R., Boxer, S.G. and Pecora, R. (1990) *Biochemistry*, **29**, 799–811.

Eimer, W. and Pecora, R. (1991) *J. Chem. Phys.*, **94**, 2324–2329.

Elias, J.G. and Eden, D. (1981) *Biopolymers*, **20**, 2368.

Fujimoto, B.S., Miller, J.M., Ribeiro, N.S. and Schurr, J.M. (1994) *Biophys. J.*, **67**, 304–308.

Gibbs, S.J. and Johnson Jr., C.S. (1991) *J. Magn. Reson.*, **93**, 395–402.

Griffiths, L. and Horton, R. (1990) *J. Magn. Reson.*, **90**, 254–263.

Hahn, E.L. (1950) *Phys. Rev.*, **80**, 580–594.

Harned, H.S. and Owen, B.B. (1958) *The Physical Chemistry of Electrolytic Solutions*, Reinhold, New York, NY, U.S.A., pp. 236–242.

Hearst, J.E. (1963) *J. Chem. Phys.*, **38**, 1062–1065.

Heus, H.A. and Pardi, A. (1991) *Science*, **253**, 191–194.

Kellomaki, A. (1975) *Finn. Chem. Lett.*, 51–54.

Kuchel, P.W. and Chapman, B.E. (1991) *J. Magn. Reson.*, **94**, 574–580.

Kuchel, P.W. and Chapman, B.E. (1993) *J. Magn. Reson.*, **101**, 53–59.

Longsworth, L.G. (1960) *J. Phys. Chem.*, **64**, 1914–1917.

Mandelkern, M., Elias, J.G., Eden, D. and Crothers, D.M. (1981) *J. Mol. Biol.*, **152**, 153–161.

Marky, L.A. and Breslauer, K.J. (1987) *Biopolymers*, **26**, 1601–1620.

Milligan, J.F., Groebe, D.R., Witherall, G.W. and Uhlenbeck, O.C. (1987) *Nucleic Acids Res.*, **15**, 8783–8798.

Natarajan, G. (1989) *Data Book on the Viscosity of Liquids*, Hemisphere, New York, NY, U.S.A.

Price, W.S. and Kuchel, P.W. (1991) *J. Magn. Reson.*, **94**, 133–139.

Sen, D. and Gilbert, W. (1992) *Biochemistry*, **31**, 65–70.

Sich, C., Flemming, J., Ramachandran, R. and Brown, L.R. (1996) *J. Magn. Reson.*, **B112**, 275–281.

Stejskal, E.O. and Tanner, J.E. (1965) *J. Chem. Phys.*, **42**, 288–292.

Tanner, J.E. (1970) *J. Chem. Phys.*, **52**, 2523–2526.

Tirado, M.M. and Garcia de la Torre, J. (1979) *J. Chem. Phys.*, **71**, 2581–2587.

Tirado, M.M. and Garcia de la Torre, J. (1980) *J. Chem. Phys.*, **73**, 1986–1993.